Journal of Materials Chemistry A

PAPER

Cite this: J. Mater. Chem. A, 2014, 2, 20237

# Aluminum–air battery based on an ionic liquid electrolyte†

D. Gelman,‡[ab] B. Shvartsev‡[b] and Y. Ein-Eli*[ab]

Received 10th September 2014
Accepted 15th October 2014

DOI: 10.1039/c4ta04721d

www.rsc.org/MaterialsA

Metal–air batteries, and particularly aluminum–air (Al–air) batteries, draw a major research interest nowadays due to their high theoretical energy content of Al (gravimetric and volumetric). Nevertheless, the implementation of Al–air batteries as a sustainable energy storage device is hampered by severe hurdles. Al anode high corrosion rate in aqueous alkaline solution is of major concern in terms of Al usage and safety. In non-aqueous electrolytes adverse Al surface activation substantially limits any power output. This study presents a novel non-aqueous Al–air battery. This battery utilizes 1-ethyl-3-methylimidazolium oligo-fluoro-hydrogenate ($EMIm(HF)_{2.3}F$) room temperature ionic liquid (RTIL). Al–air batteries can sustain current densities up to 1.5 mA $cm^{-2}$, producing capacities above 140 mA h $cm^{-2}$, thus utilizing above 70% of the theoretical Al capacity. This is equivalent to an outstanding energy densities of 2300 W h $kg^{-1}$ and 6200 W h $L^{-1}$. We detected $Al_2O_3$ at the air electrode as the battery discharge product of the oxygen reduction coupled with Al ions migrated to the air electrode.

## Introduction

The changing and expanding needs in the energy market, ranging from power grid energy storage systems to portable power sources, dictates the development of efficient, inexpensive, and high performance battery systems. These advanced electrochemical systems should confront with the challenges posed by the nascent green economy and non-oil based transport systems. A promising path for achieving these goals is the development of aluminum (and its alloys) based battery systems. The main advantages of such systems are the low equivalent weight of Al, its high natural abundance in the earth's crust (leading to a rather low price), and its safety characteristics. Additionally, Al and its by-products are non-toxic and environmental friendly.[1,2] Aluminum battery systems cover a wide range of applications; from field-portable emergency power supply to remote power applications and batteries for transportation.[1] Theoretically, Al contains approximately half of gasoline energy content per unit weight (8100 W h $kg^{-1}$ for Al–air[1,3] and 13 000 W h $kg^{-1}$ for gasoline[4]) and three times the energy per unit volume (21 870 W h $L^{-1}$ for Al–air[3] and 9700 W h $L^{-1}$ for gasoline[5]). Currently, the best practical utilization of gasoline for automotive applications can approach 1700 W h $kg^{-1}$ (ref. 4) while for aqueous Al–air batteries it is 300–500 W h $kg^{-1}$.[3]

Metal–air battery systems utilize an active metal as an anode (fuel) and carbonaceous materials as the cathode with ambient oxygen as the cathodic material. These batteries are classified according to the anode metal type, since air (oxygen) is a common feature.[1,2] Aqueous Al–air batteries have been reported as early as 1960's and the main effort up to date has focused on two aqueous electrolyte types: alkaline and saline.[1,2] Thermodynamically, Al anode exhibit a potential of −1.66 V in saline and −2.35 V in alkaline electrolyte.[1] However, practical Al electrodes operate at significantly lower potentials, since Al is normally covered with an oxide/hydroxide film, causing a voltage-delay. Moreover, Al anode experiences a considerable parasitic corrosion reaction in aqueous solutions. This results in a substantial low Al utilization (degraded coulombic efficiency), accompanied by a massive hydrogen gas evolution.[1] Another concern relates to electrolyte imbalance during cell discharge: on one hand, progressive consumption of hydroxyl ions occurs at the Al electrode; on the other hand, the electrolyte progressively saturates with aluminate. Eventually, aluminate concentration exceeds the super-saturation, a crystalline form of aluminum hydroxide precipitates, and therefore loss of the ionic conductivity of the solution.[1]

The current study, to the best of our knowledge, is the first report on an Al–air battery utilizing a non-aqueous electrolyte. In this specific case study a Room Temperature Ionic Liquid (RTIL) was implemented. The unique properties of the hydrophilic 1-ethyl-3-methylimidazolium oligo-fluoro-hydrogenate ($EMIm(HF)_{2.3}F$) allow Al electrochemical dissolution, on one hand, and efficient oxygen reduction, on the other hand (as previously reported in Si–air battery systems[6,7] and fuel cells[8]), without any parasitic corrosion degradation. Thus, the above

[a]The Nancy and Stephen Grand Technion Energy Program, Technion-Israel Institute of Technology, Haifa, Israel 3200003. E-mail: eineli@tx.technion.ac.il

[b]Department of Materials Science and Engineering, Technion-Israel Institute of Technology, Haifa, Israel 3200003

† Electronic supplementary information (ESI) available. See DOI: 10.1039/c4ta04721d

‡ Equally contributed to the presented study.

provides a synergistic effect in this appealing high energy power source. Additionally, a substantial water addition to the $EMIm(HF)_{2.3}F$ does not hamper Si–air battery performance, but rather leads to an increase in the cell discharge capacity.[9]

RTILs – room temperature molten salts – are composed mostly of organic ions and are *inter alia* used as the electrolyte of choice in batteries[2,10] and other energy conversion systems.[11–13] Ionic liquid electrolytes are advantageous compared to aqueous electrolytes, as aluminum is not prone to the parasitic hydrogen generation reaction.[14] Several researchers explored the possible use of chloroaluminate ionic liquids as electrolytes in aluminum based batteries.[2] A drawback of chloroaluminate ionic liquids is the difficulty to produce them, as the reaction between 1-ethyl-3-methyl-imidazolium chloride (EMIC) and $AlCl_3$ is highly exothermic.[2,15,16] Additionally, chloroaluminate ionic liquids react rapidly and exothermally with moister.[17] An alternative to chloroaluminate ionic liquids is air and water stable ionic liquids. Although various RTILs were already synthesized and studied {for example 1-ethyl-3-methylimidazolium bis-(trifluoro-methyl-sulfonyl)amide ([EMIm]TFSI),1-butyl-1-methyl-pyrrolidinium bis-(trifluoro-methyl-sulfonyl)imide ([BMP]TFSI), [(trihexl-tetradecyl)phosphonium] bis-(trifluoro-methyl-sulfonyl)imide ($P_{14,6,6,6}$TFSI)[18,19] and 1-butyl-3-methyl-imidazolium tetra-fluoroborate, [BMIm]TFB[20]}, non-aqueous Al-ion battery research is still in its initial stages.[21–23] The bottle-neck for further progress are both the rather poor Al cathode potential and its very low gravimetric capacity. Thus, using the above mentioned RTIL electrolytes in Al–air battery failed. Moreover, in comparison to Li–$O_2$ batteries, which were heavily investigated mainly in pure $O_2$ environments,[24–27] the reported Al–air system operated in atmospheric air.

We chose $EMIm(HF)_{2.3}F$ as the electrolyte in our Al–air battery system, since previous reports demonstrated the use of this RTIL in Si–air batteries.[6,7] Among its fascinating properties, one may include ultra-high conductivity (100 mS $cm^{-1}$, one of the highest among RTILs), low viscosity and chemical stability with oxygen and water.[7,28]

# Experimental

### Materials and chemicals

1-ethyl-3-methyl-imidazolium-oligo-flouro-hydrogenat, $EMIm(HF)_{2.3}F$, (Boulder Ionics, Inc.) was used without further purification. For both anodic and cathodic performances studies, a three-electrode configuration was used, with Al foil (0.25 mm thick 99.997%, Alfa Aesar), serving as the working electrode in anodic polarization measurements and porous carbon-based air electrode (Electric Fuel, Inc.) for the cathodic polarization experiments (it is important to note that the air cathode was formulated to alkaline Zn–air). The air electrode had surface area of 533 $m^2$ $g^{-1}$, average pore diameter of 5.43 nm and carbon loading of 19 mg $cm^{-2}$. The air electrode was composed of 6.6% wt $MnO_2$ catalyst dispersed in 77% wt activated carbon powder and 16.4% wt PTFE, as a binder.

### Three electrodes cell preparation

Three electrodes cell configuration was used, with an Al foil or air electrode serving as the working electrode, platinum foil was used as a counter electrode and $Fc/Fc^+$ (ferrocene/ferrocenium ion) gel based was utilized as a reference electrode.[29] The experiments were carried out in a polypropylene electrochemical cell with an exposed surface area of 1.13 $cm^2$ with nickel metal (98%, Spectrum) connectors (as shown in Fig. S1 in the ESI†). Prior to any experiment, the Al electrode was cleaned in ethanol, acetone and then air dried. No pretreatment was applied to the air electrode.

### Two electrode cell preparation

In full battery studies (two electrode configuration), similar cell structure (to the three electrode cell) was used but without the introduction of reference electrode (Fig. S1†). Al foil and air cathode were utilized as the electrodes, with the same pretreatment as previously described. The cells were held at OCP (open circuit potential) in all the electrochemical experiments for 4 hours prior to initiating the discharge process. This was performed in order to allow a proper wetting of the porous carbon (at the air cathode) with the RTIL electrolyte.

### Electrochemical measurements and characterization

Potentiodynamic and linear polarization (corrosion current measurement) experiments were performed with a VersaSTAT Princeton Applied Research potentiostat/galvanostat. Full battery discharge experiments were performed using an Arbin BT2000 battery test system. All experiments (if not mentioned otherwise) were conducted in ambient air. Airless experiments were conducted in an Ar-filled glove box (MBraun Unilab, $H_2O$ and $O_2$ below 1 ppm). Surface morphology was obtained by HRSEM (Zeiss Ultra-Plus FEG-SEM) and by SEM (FEI E-SEM Quanta 200, equipped with EDS). Surface analysis of the air electrode was conducted by XPS (Thermo VG Scientific, Sigma probe, GB). Details on XPS studies and description of the experimental conditions and peaks assignment and identification[30] can be found in the ESI† – Section 2.

# Results and discussion

### Half-cell analysis

Preliminary half-cell configuration experiments were conducted using the proposed Al/$EMIm(HF)_{2.3}F$/air battery system. The potentiodynamic measurements (shown in Fig. 1) provide data on possible battery cell potential and the effective current densities expected in such configurations. Open circuit potential (OCP) values of both the Al (anode) and air electrodes (cathode) indicate that the expected rest potential of the Al–air cell is $\Delta V = 2.1$ V (marked in Fig. 1). In addition, the expected current densities of both Al anode and air electrode cathode are in the range of a few milliamperes (mA). These results suggest that the proposed couple in the electrolyte may indeed function as a battery.

It is well known that aluminum undergoes an extremely fast corrosion process in alkaline solutions.[1,2,31] Aluminum

 

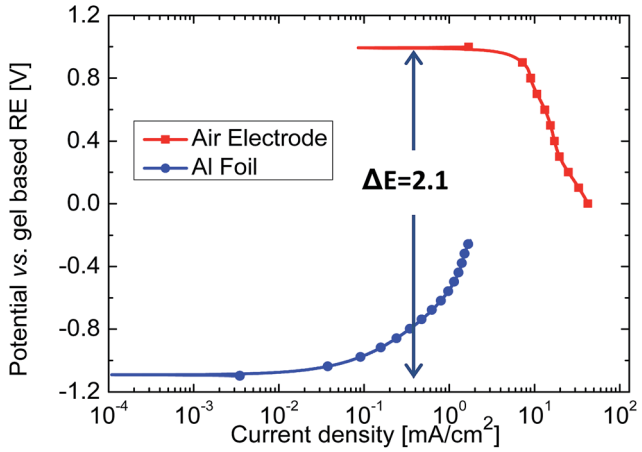


Fig. 1 Potentiodynamic measurements conducted at a scan rate of 5 mV $s^{-1}$ with the air electrode (cathodic polarization, red squares) and the Al anode (anodic polarization circle, blue circles) *vs.* $Fc/Fc^{+}$ gel based reference electrode.

corrosion currents usually are in the order of $10^{1}$ to $10^{2}$ [mA $cm^{-2}$][31] and therefore, high rates of self-discharge processes are expected. Aluminum corrosion current of 25 [μA $cm^{-2}$] in $EMIm(HF)_{2.3}F$ RTIL electrolyte, has been obtained *via* linear polarization experiments (±20 mV relative to OCP). Generally, the results show high stability and negligible corrosion rates for aluminum in $EMIm(HF)_{2.3}F$.

### Aluminium–air cell discharge performance

Following the half-cell studies, a full battery discharge was performed for different current densities at ambient temperature of 23 ± 2 °C and atmospheric air (Fig. 2a). Similar discharge experiment was performed with an identical cell in an inert atmosphere (Ar gas) glove box at a current density of 0.5 [mA $cm^{-2}$] (Fig. 2b). This experiment was performed to reassure that the relevant cathodic electrochemical reaction indeed involves atmospheric oxygen. As presented in Fig. 2a, Al–air cell was discharged in rates ranging from 0.1 to 1.5 [mA $cm^{-2}$]. The battery has the ability to support current densities as high as 1.5 mA $cm^{-2}$ and possibly even higher. Moreover, the cell that was discharged in airless conditions at the Ar glove box (Fig. 2b) did not sustain a working potential and failed under the applied current. This strongly indicates that the cathodic reaction involves oxygen reduction. Additionally, the initial potential drop after 4.5 hours from cell activation (Fig. 2a), observed in most discharge profiles, may suggest a layer formation on the Al/electrolyte interface. The presence of such a layer may be attributed to a possible surface modification of the Al, as a segment of the interaction with the ionic liquid; most probably, the anionic species in the electrolyte reacts with the Al to produce $AlF_x$ terminated surface (see Fig. S2 in ESI†). The origin of such potential drop at the early stages of the discharge may also be attributed to the air cathode itself; insufficient rest time for a properly air cathode wetting was posed by restricting the rest step to 4 hours, prior to cell operation.

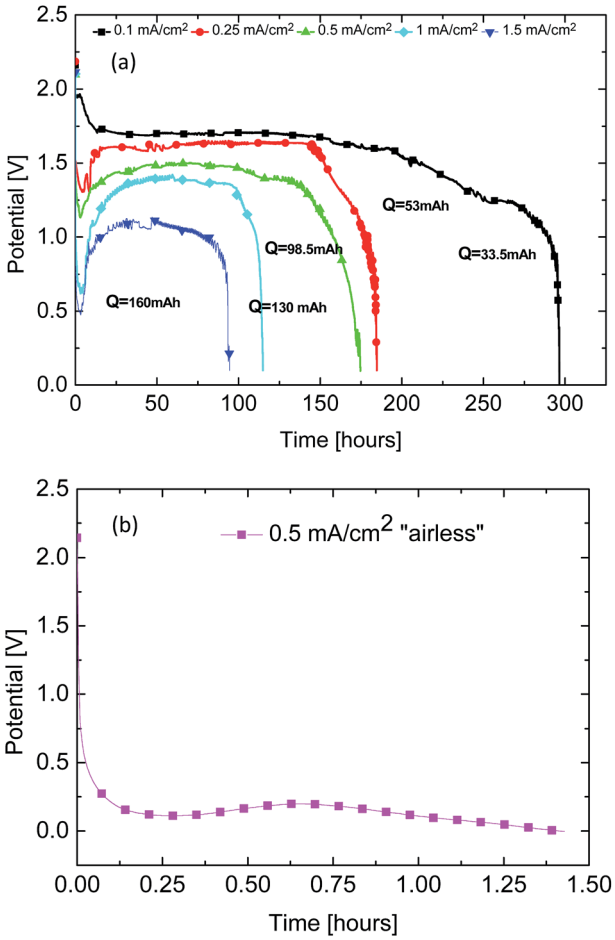


Fig. 2 (a) Al–air battery discharge profiles at different current densities of 0.1 (black square); 0.25 (red circle); 0.5 (green up-based triangle); 1 (cyan diamond) and 1.5 mA $cm^{-2}$ (blue down-based triangle). (b) Al–air cell discharge (0.5 mA $cm^{-2}$ square, magenta) in an inert atmosphere (airless).

From the presented discharge results (Fig. 2a) up to 70% of Al utilization was achieved during cells discharge. The capacities associated with cell discharge (up to 160 mA h being equivalent to 140 mA h $cm^{-2}$) are extremely high, compared to the theoretical capacity of the Al electrode (calculated to be 227 mA h, equivalent to 200 mA h $cm^{-2}$ [see ESI† (Section 4) for detailed capacity calculations]).

### Electrode surface analyses

Following the electrochemical study, a surface morphology characterization of the Al anode was conducted with the use of high resolution scanning electron microscope (HRSEM) and is being presented in Fig. 3. The morphology of the Al changes dramatically as a function of the applied current. At lower current densities (0.1 mA $cm^{-2}$) small diameter pores (20–50 nm), are visible (Fig. 3b and c). At higher current densities, as may be expected, larger pores (200–400 nm) are visible. This may be attributed to aluminum electrochemical dissolution rate reaction: at higher current densities, rapid dissolution occurs, leading to surface coarsening.

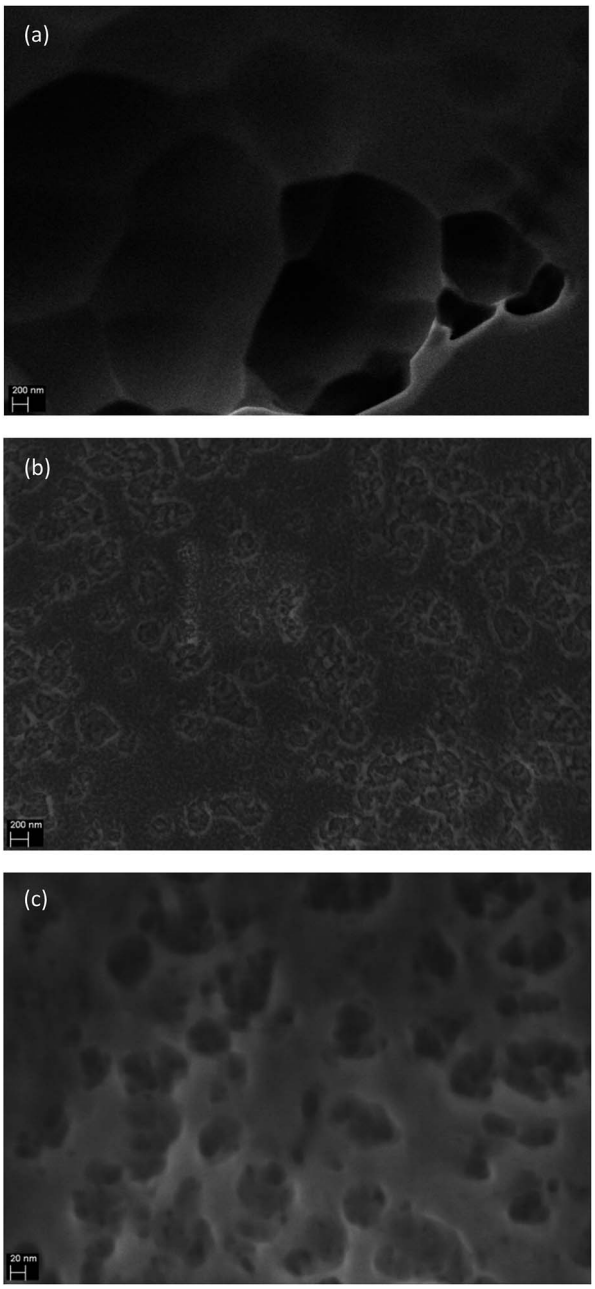


Fig. 3 (a–c) HRSEM micrographs of Al anode surface after discharge at (a) 1.5 mA $cm^{-2}$ and (b and c) at 0.1 mA $cm^{-2}$.

The analysis of the cathode surface was also conducted as presented in Fig. 4. The figure presents X-ray photoelectron spectroscopy (XPS, Fig. 4a) and morphological (SEM, Fig. 4b–d) results obtained for the air cathode prior and subsequent to discharge in two different current densities, 0.5 mA $cm^{-2}$ and 1.5 mA $cm^{-2}$.

In order to identify the chemical nature of the deposits, XPS analysis was also conducted (Fig. 4a). The Al 2p spectrum signal can be de-convoluted into two separated peaks at 74–75 eV ($Al_xO_y$ species) and at 70–71 eV (metallic aluminum). The only peak obtained subsequent to the Al–air battery discharging is of $Al_xO_y$ species, while no metallic peak of Al was recorded. One

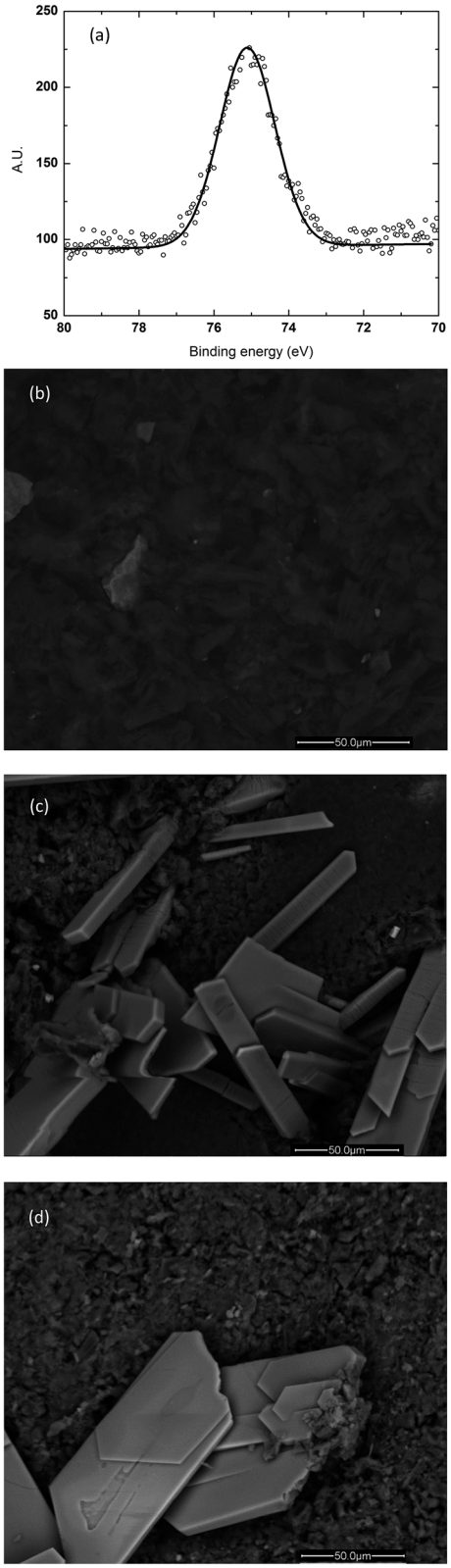


Fig. 4 (a) XPS measurement of the air electrode after discharge at 1.5 mA $cm^{-2}$. (b–d) Back-scattered electrons (BSE) SEM micrographs of air cathode electrode surface; (b) pristine air electrode (c) after discharge at 0.5 mA $cm^{-2}$, (d) after discharge at 1.5 mA $cm^{-2}$.

can conclude that during Al–air battery operation, $Al_xO_y$ species (most probably $Al_2O_3$) are formed at the cathode side, as the final product of the reaction between reduced oxygen and oxidized Al at the air electrode.

In general, the cell reaction may be postulated as:

$$4Al + 3O_2 \rightarrow 2Al_2O_3 \quad (1)$$

The specific reaction of both the Al anode (oxidation) and the oxygen (reduction) at the air electrode is still to be determined exactly.

Comparing the pristine air electrode (Fig. 4b) and air electrode following a battery discharge (Fig. 4c, 0.5 mA $cm^{-2}$ and Fig. 4d, 1.5 mA $cm^{-2}$) it is evident that in the course of cell operation a deposition process of by-products occurred. The deposits are in a form of elongated facets in the μm scale as clearly seen in Fig. 4c and d. A clear difference in the size and distribution of the products is visible as a function of the discharge current density. For lower current density (Fig. 4c, 0.5 mA $cm^{-2}$) smaller and densely dispersed particles are shown, when for the higher current density (Fig. 4d, 1.5 mA $cm^{-2}$) fewer and larger products are visible.

The differences in the products morphology may explain the behavior of the capacity as a function of the current density; in higher current densities larger capacity was measured (Fig. 2a). The phenomenon was already recorded for Si–air batteries applying the same electrolyte and air cathode.[7] This specific behavior was attributed to differences in the morphology of the discharge products at the cathode/electrolyte interface, leading to micro-pores blocking effects at the air cathode pores. As suggested, high current densities discharge would lead to the formation of coarse and bulky deposits, while cell discharge processes in lower current densities would produce finer oxides deposits at the air cathode, blocking further possible oxygen reduction at these sites and thus terminating the discharge prematurely.

### Comparison to other metal air battery systems

In Table 1 different figures of merits of the new Al–air battery and compare the performance of this unique cell with other metal–air batteries such as aqueous Zn–air and Al–air batteries and the Li–air battery system, currently being heavily investigated. For the sake of a proper comparison between the systems, only data collected at ambient conditions were taken into account (room temperature discharge at atmospheric air, without any oxygen feed). It is evident that the cell energy density (both volumetric and gravimetric) of the new non-aqueous Al–air battery system is most appealing, having ~2300 W h $kg^{-1}$ and ~6200 W h $L^{-1}$ (when actually the cell capacity is limited by the anodic material).

The values recorded and reported for the other 3 metal–air batteries are substantially lower, by at least a factor of 2–3. Additionally, low to almost negligible corrosion rates of the Al anode in the RTIL renders the proposed system highly attractive in terms of high electrode utilization. In addition, the expected practical values in a battery configuration (taking into account all battery active materials and elements, namely Al anode, air electrode and electrolyte without battery packing materials) are expected to be 925 W h $kg^{-1}$ and 1692 W h $L^{-1}$ (the reader is referred to ESI,† Section 4.3). Aluminum corrosion current in $EMIHF_{2.3}F$ (serving as indicative for the battery self-discharge), was measured with the application of a linear polarization method. The Al anode possesses corrosion currents that are lower by three orders of magnitude, compared to Al immersed in alkaline. Interestingly, the yet unmodified Al anode immersed in the ionic liquid shows quite low corrosion rate, as Zn anode does once immersed in alkaline media. Needless to state that the Zn anode is routinely being modified by corrosion mitigation alloying elements, as well as by inhibitors being added to the alkaline solution.[31] It is also striking that the reported Al–air battery system is surpassing the most researched Li–air battery system, having substantially lower energy densities (especially volumetric one). Thus, the values being reported here on the Al–air system are by far better than any metal–air battery so far reported. Contrary to other metal–air battery electrolytes, the ionic liquid electrolyte exhibits extremely high tolerance to environmental conditions (such as high and low relative humidity and exposure to air), as reported elsewhere.[19]

## Conclusions

We reported here for the first time of a non-aqueous, ionic liquid electrolyte based Al–air battery. The proposed cell configuration displayed an outstanding capacity performance: up to 70% utilization of the metallic Al theoretical capacity with energy density exceeding any reported metal–air battery system. Analysis of the Al–air battery components subsequent to a complete cell discharge indicated the presence of $Al_2O_3$ at the air cathode and active dissolution at the Al anode surface.

Table 1 Parameters comparison between 4 different metal–air batteries; Zn–, Al– (aqueous), Li– and Al– (non-aqueous) air battery systems

| Battery system | Practical gravimetric energy density[a] [W h $kg^{-1}$] | Practical volumetric energy density[a] [W h $L^{-1}$] | Corrosion current [μA $cm^{-2}$] |
|---|---|---|---|
| Zn–air | 300 (ref. 3 and 32) | 2150 | 30[b] (ref. 31) |
| Al–air (aqueous) | 500 (ref. 3 and 31) | 1350 | 9900[b] (ref. 32) |
| Li–air | 362 (ref. 33 and 34) | 194 | 4.3[b] (ref. 34) |
| Al–air (non-aqueous) | 2300 | 6200 | 25 |

[a] Cell capacity was calculated based on active metal weight and volume. [b] High sensitivity to low/high relative humidity and severe reaction with atmospheric $CO_2$.

An additional extensive research should be conducted studying the new non-aqueous Al–air battery system, *i.e.* seeking appropriate conditions to further develop this Al–air battery into a rechargeable one, allowing reversible and efficient charge–discharge cycles. Among the crucial parameters to be further investigated are the ionic liquid type, in terms of formulation and conductivity, feasibility of reversible oxygen reduction/oxidation reactions, as well as reversible and efficient Al stripping and deposition processes in the formulated electrolyte.

## Acknowledgements

This work was supported by the Israeli Science Foundation (ISF) Grant no. 1701/12, by Israel National Center for Electrochemical Propulsion (INREP-ISF) and by Grand Technion Energy Program (GTEP). The authors would like to thank Itamar Wallwater for his part and his help in the execution of the experiments.

## Notes and references

1 Q. Li and N. J. Bjerrum, *J. Power Sources*, 2002, **110**, 1–10.
2 D. Egan, C. Ponce de León, R. Wood, R. Jones, K. Stokes and F. Walsh, *J. Power Sources*, 2013, **236**, 293–310.
3 S. Yang and H. Knickle, *J. Power Sources*, 2002, **112**, 162–173.
4 G. Girishkumar, B. McCloskey, A. Luntz, S. Swanson and W. Wilcke, *J. Phys. Chem. Lett.*, 2010, **1**, 2193–2203.
5 G. Pistoia, *Lithium-Ion Batteries: Advances and Applications*, Newnes, 2013.
6 G. Cohn, D. Starosvetsky, R. Hagiwara, D. D. Macdonald and Y. Ein-Eli, *Electrochem. Commun.*, 2009, **11**, 1916–1918, DOI: 10.1016/j.elecom.2009.08.015.
7 G. Cohn and Y. Ein-Eli, *J. Power Sources*, 2010, **195**, 4963–4970, DOI: 10.1016/j.jpowsour.2010.02.070.
8 R. Hagiwara, T. Nohira, K. Matsumoto and Y. Tamba, *Electrochem. Solid-State Lett.*, 2005, **8**, A231–A233.
9 G. Cohn, D. D. MacDonald and Y. Ein-Eli, *ChemSusChem*, 2011, **4**, 1124–1129, DOI: 10.1002/cssc.201100169.
10 M. Armand, F. Endres, D. R. MacFarlane, H. Ohno and B. Scrosati, *Nat. Mater.*, 2009, **8**, 621–629.
11 V. Di Noto, S. Lavina, G. A. Giffin, E. Negro and B. Scrosati, *Electrochim. Acta*, 2011, **57**, 4–13.
12 V. D. Noto, M. Piga, G. A. Giffin, S. Lavina, E. S. Smotkin, J. Sanchez and C. Iojoiu, *J. Phys. Chem. C*, 2012, **116**, 1361–1369.
13 V. Di Noto, M. Piga, G. A. Giffin, S. Lavina, E. S. Smotkin, J. Sanchez and C. Iojoiu, *J. Phys. Chem. C*, 2012, **116**, 1370–1379.
14 S. Licht, G. Levitin, R. Tel-Vered and C. Yarnitzky, *Electrochem. Commun.*, 2000, **2**, 329–333.
15 T. Jiang, M. Chollier Brym, G. Dubé, A. Lasia and G. Brisard, *Surf. Coat. Technol.*, 2006, **201**, 1–9.
16 Y. Zhao and T. VanderNoot, *Electrochim. Acta*, 1997, **42**, 3–13.
17 T. Tsuda and R. Hagiwara, *J. Fluorine Chem.*, 2008, **129**, 4–13.
18 S. Zein El Abedin, E. Moustafa, R. Hempelmann, H. Natter and F. Endres, *ChemPhysChem*, 2006, **7**, 1535–1543.
19 T. Kuboki, T. Okuyama, T. Ohsaki and N. Takami, *J. Power Sources*, 2005, **146**, 766–769.
20 J. Wang, J. Wang, H. Shao, X. Zeng, J. Zhang and C. Cao, *Mater. Corros.*, 2009, **60**, 977–981.
21 N. Jayaprakash, S. K. Das and L. A. Archer, *Chem. Commun.*, 2011, **47**, 12610–12612.
22 J. V. Rani, V. Kanakaiah, T. Dadmal, M. S. Rao and S. Bhavanarushi, *J. Electrochem. Soc.*, 2013, **160**, A1781–A1784.
23 W. Wang, B. Jiang, W. Xiong, H. Sun, Z. Lin, L. Hu, J. Tu, J. Hou, H. Zhu and S. Jiao, *Sci. Rep.*, 2013, **3**, 3383.
24 R. Choi, J. Jung, G. Kim, K. Song, Y. Kim, S. C. Jung, Y. Han, H. Song and Y. Kang, *Energy Environ. Sci.*, 2014, **7**, 1362–1368.
25 F. Li, D. Tang, Z. Jian, D. Liu, D. Golberg, A. Yamada and H. Zhou, *Adv. Mater.*, 2014, **26**, 4659–4664.
26 F. Li, Y. Chen, D. Tang, Z. Jian, C. Liu, D. Golberg, A. Yamada and H. Zhou, *Energy Environ. Sci.*, 2014, **7**, 1648–1652.
27 D. Wu, Z. Guo, X. Yin, Q. Pang, B. Tu, L. Zhang, Y. Wang and Q. Li, *Adv. Mater.*, 2014, **26**, 3258–3262.
28 R. Hagiwara, T. Hirashige, T. Tsuda and Y. Ito, *J. Electrochem. Soc.*, 2002, **149**, D1–D6.
29 B. Shvartsev, G. Cohn, H. Shasha, R. Eichel and Y. Ein-Eli, *Phys. Chem. Chem. Phys.*, 2013, **15**, 17837–17845.
30 D. Gelman, D. Starosvetsky and Y. Ein-Eli, *Corros. Sci.*, 2014, **82**, 271–279.
31 M. Doche, J. Rameau, R. Durand and F. Novel-Cattin, *Corros. Sci.*, 1999, **41**, 805–826.
32 M. Auinat and Y. Ein-Eli, *J. Electrochem. Soc.*, 2005, **152**, A1158.
33 A. Kraytsberg and Y. Ein-Eli, *J. Power Sources*, 2011, **196**, 886–893.
34 J. Cessna, *Corrosion*, 1971, **27**, 244–254.

 